Direct Time-Resolved and Spatially Resolved Monitoring of Molecular Transport in a Crystalline Nanochannel System

Javier Marti-Rujas,[†] Arnaud Desmedt,[‡] Kenneth D. M. Harris,*,[†] and François Guillaume*,[‡]

School of Chemistry, Cardiff University, P.O. Box 912, Cardiff CF10 3TB, Wales, and Laboratoire de Physico Chimie Moléculaire, UMR CNRS 5803, Université de Bordeaux 1, 351 cours de la Libération, 33405 Talence Cedex, France

Received April 23, 2004; E-mail: harriskdm@cardiff.ac.uk; f.guillaume@lpcm.u-bordeaux1.fr

Many important processes, including those of biological,[1] industrial,[2] and nanotechnological[3] interest, rely upon the transport of molecules or ions through channel systems. Although details of the transport process clearly differ from one system to another, well-defined model systems have an important role to play in furnishing a general fundamental understanding of such processes. In this regard, we recently demonstrated[4] the design of a molecular-scale capillary capable of selective molecular transport processes. The material is based on an incommensurate inclusion compound, in which guest molecules are contained within a system of one-dimensional channels (diameter ca. 5.5 Å) in a crystalline urea host structure[5] (Figure 1a). It was shown that the net transport of guest molecules in one direction along the channel system can be achieved by inserting new guest molecules at one end of the crystal (by putting it in contact with the liquid of another potential guest), with the original guest molecules expelled from the other end. Such phenomena have considerable potential in a number of applications, including selective nanoscale separation techniques based on discrimination of molecular size, shape, and chirality. As discussed previously,[4] one feature of the incommensurate nature[5b,6] of the inclusion compounds studied is that the activation barrier to diffusion along the channel should be very low (although clearly the insertion of molecules at one end of the channel and the expulsion of molecules at the other end should be associated with activation barriers that are not negligible).

While the occurrence of this transport process was demonstrated on the basis of visual observation, chemical analysis, and X-ray diffraction, our previous studies did not investigate the spatial distribution of the two types of guest molecule within the crystal nor the variation of the spatial distribution of the guest molecules as a function of time. To address these issues, the present communication demonstrates that confocal Raman microspectrometry[7] can be used successfully as an in situ probe of the transport process, yielding information on the spatial distribution of guest molecules and its time dependence. Although several different combinations of guest molecules are of interest, we focus here on the system in which the "original" and "new" guest molecules are 1,8-dibromooctane (DBO) and pentadecane (PD), respectively, as the C−Br stretching vibration can be used to assess the relative amount of DBO guest molecules as a function of position and time within the channel system.

Single crystals[8] of the DBO/urea inclusion compound were prepared using standard procedures.[9] The laboratory reference frame in our Raman experiments[10] is defined in Figure 1, with the Z axis collinear to the direction of the incident laser beam. The direction of polarization of the incident laser beam defines the X axis. The scattered light was collected in the same direction as the incident
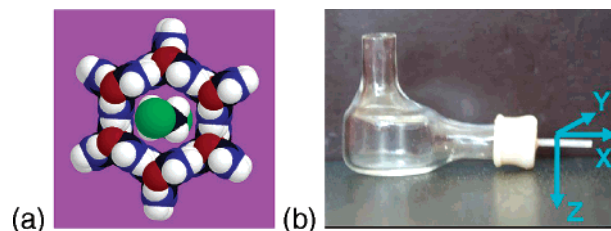

Figure 1. (a) Structure of a single tunnel in the DBO/urea inclusion compound (with van der Waals radii and arbitrary orientation of the DBO guest molecule). (b) Experimental assembly comprising the urea inclusion compound crystal (right) and reservoir containing liquid PD (left). The orientation of the crystal relative to the laboratory reference frame (X, Y, Z) is shown.

light (backscattering geometry), and was analyzed through a polarizer along the X component. To monitor the transport process, a single crystal of DBO/urea was attached (using septum and Araldite as a sealing system) to a reservoir containing liquid PD (Figure 1b). The long axis (channel direction) of the needle-shaped crystal was aligned parallel to the X axis of the reference frame, and polarized spectra ($Z(XX)\bar{Z}$ in Porto notation[11]) were recorded.

The DBO/urea single crystal and reservoir of liquid PD were mounted on an X,Y-motorized microscope table.[12] Increasing positive values of X correspond to the direction of transport of PD. Spectra were recorded by scanning a rectangular slice of length 5200 μm (along X) by width 600 μm (along Y) at a fixed depth of 175 μm below the top surface of the crystal (along Z). The time to record the entire Raman image of the probed area was about 28 min.

Polarized Raman spectra of α,ω-dibromoalkane/urea and alkane/urea inclusion compounds studied previously[13] allow us to establish the Raman peaks that are useful for monitoring the transport process. The C−Br stretching vibration ν(CBr) of DBO (which adopts mainly the all-trans conformation within the urea channel) gives an intense $Z(XX)\bar{Z}$ polarized peak at about 620 cm^{-1} (Figure 2a), whereas the methyl rocking vibration r(CH$_3$) for the all-trans PD is at ca. 900 cm^{-1} (Figure 2b). The Raman bands of the urea host structure are identical for both the DBO/urea and PD/urea inclusion compounds.[14] In particular, the symmetric C−N stretching vibration ν_s(CN) of urea gives a very intense $Z(XX)\bar{Z}$ polarized Raman band at 1024 cm^{-1} (Figure 2a,b). Thus, variation in the amount of DBO guest molecules in a single crystal can be probed by measuring the ratio $R = I(CBr)/I(CN)$ of the integrated intensities [denoted I(CBr) and I(CN), respectively] of the ν(CBr) and ν_s(CN) Raman bands. In this way, the transport process may be evaluated by measuring R as a function of position in the crystal. In practice, we use a normalized ratio $\langle R \rangle = R/R_0$, where R_0 is the value of R (averaged over the probed area) for the original crystal of DBO/ urea (before starting the transport process). Thus, $\langle R \rangle = 1$ if the
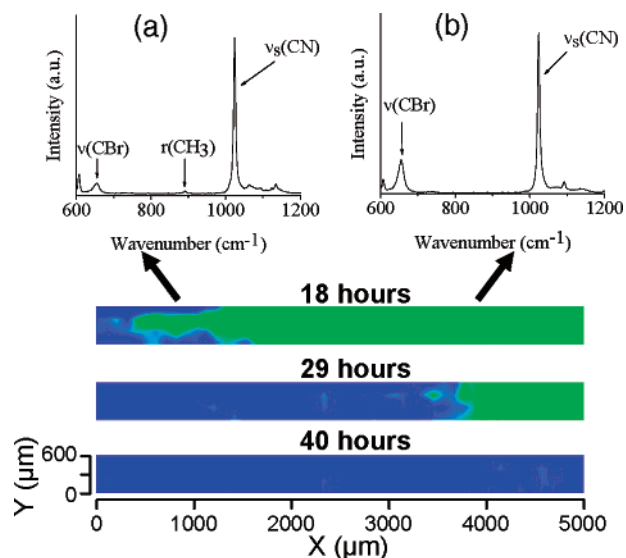
Figure 2. Raman spectra recorded during the transport process (at 18 h) for (a) a region of the crystal containing both DBO and PD guest molecules and (b) a region containing only DBO guest molecules. The lower figures show the variation in $\langle R \rangle$ for the imaged region of the crystal at different times after commencement of the transport process (green: DBO-rich regions, $\langle R \rangle \geq 0.5$; blue: PD-rich regions, $\langle R \rangle < 0.5$). Quantitative information on the spatial distribution $\langle R \rangle$ is given in Figure 3.

inclusion compound contains only DBO guest molecules, and $\langle R \rangle = 0$ if it contains only PD guest molecules.

The occurrence of molecular transport inside the urea inclusion compound is clearly evident from Figure 2, which shows the probed area at 18, 29, and 40 h, respectively, after commencing the transport process (i.e. after one end of the crystal had been put in contact with liquid PD). At 18 h, it is clear (from consideration of the r(CH$_3$) and ν(CBr) modes) that both DBO and PD are present at the end of the crystal in contact with liquid PD ($\langle R \rangle \approx 0.3$), whereas only DBO is present at the other end of the crystal ($\langle R \rangle \approx$ 1). At 40 h, our results show that PD guest molecules are present over the full length of the crystal. Interestingly, our experiments (including studies over longer periods of time than those presented here) suggest that complete exchange does not occur, and the ratio $\langle R \rangle$ typically does not fall below 0.1. Thus, a proportion of the original DBO guest molecules are unable to take part in the exchange process, and it is reasonable to propose that transport in some channels may be impeded as a result of structural defects. Importantly, the Raman bands assigned to urea remain unchanged throughout the period of time investigated, suggesting that the urea host structure is not significantly affected by the transport process.

To assess the variation in the distribution of guest molecules as a function of time, we consider one-dimensional scans (along X) through each of the images shown in Figure 2 (with the scan taken at the same fixed Y value in each case). For each of these scans, the value of $\langle R \rangle$ is plotted as a function of X in Figure 3. An approximately sigmoidal distribution is observed, and at the earlier stages of the process (18 h), there is a comparatively narrow boundary region (with width of the order of 1000 μm) between the DBO-rich ($\langle R \rangle \approx 1$) and PD-rich ($\langle R \rangle \approx 0.3$) regions of the crystal. As time progresses, translation of the centroid of the distribution along the crystal and spreading of the boundary region are evident. It is clear that such data, recorded as a function of both position within the crystal and time, can give access to
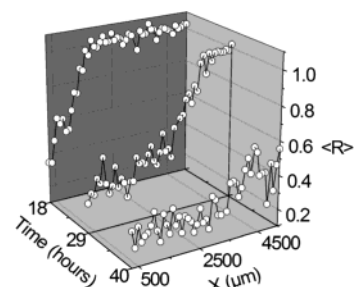

Figure 3. Plots of $\langle R \rangle$ as a function of position X along the channel direction at different times after commencement of the transport process. The same fixed Y value was used for each scan.

quantitative information on the kinetics of the transport process and the time-dependence of the spatial distribution of guest molecules within the channel system. Detailed data analysis, leading toward this information, is currently in progress, alongside experimental studies to obtain insights on other fundamental aspects of the transport process. Among these aspects, it is clear that the surface properties[15] of the crystals at the ends of the tunnels [the (001) surfaces] must have a significant bearing on the occurrence and rate of the transport process.

References

(1) (a) Preston, G. M.; Carroll, T. P.; Guggino, W. B.; Agre, P. *Science* **1992**, *256*, 385−387. (b) Doyle, D. A.; Morais Cabral, J.; Pfuetzner, R. A.; Quo, A.; Gulbis, J. M.; Cohen, S. L.; Chait, B. T.; MacKinnon, R. *Science* **1998**, *280*, 69−77.
(2) Thomas, J. M. *Angew. Chemie Int. Ed.* **1999**, *38*, 3588−3628.
(3) (a) Hod, O.; Rabani, E. *Proc. Nat. Acad. Sci.* **2003**, *100*, 14661−14665. (b) Kalra, A.; Garde, S.; Hummer, G. *Proc. Nat. Acad. Sci.* **2003**, *100*, 10175−10180. (c) Wei, C. Y.; Srivastava, D. *Phys. Rev. Lett.* **2003**, *91*, art. no. 235901.
(4) Khan, A. A.; Bramwell, S. T.; Harris, K. D. M.; Kariuki, B. M.; Truter, M. R. *Chem. Phys. Lett.* **1999**, *307*, 320−326.
(5) (a) Smith, A. E. *Acta Crystallogr.* **1952**, *5*, 224−235. (b) Harris, K. D. M.; Thomas, J. M. *J. Chem. Soc. Faraday Trans.* **1990**, *86*, 2985−2996. (c) Hollingsworth, M. D.; Harris, K. D. M. in *Comprehensive Supramolecular Chemistry* (MacNicol, D. D., Toda, F., Bishop, R., Eds.), Pergamon Press: **1996**, Volume *6*, p 177−238.
(6) (a) Rennie, A. J. O.; Harris, K. D. M. *Proc. Royal Soc. A* **1990**, *430*, 615−640. (b) Lefort, R.; Etrillard, J.; Toudic, B.; Guillaume, F.; Breczewski, T.; Bourges, P. *Phys. Rev. Lett.* **1996**, *77*, 4027−4030.
(7) Bruneel, J. L.; Lassègues, J. C.; Sourisseau, C. *J. Raman Spectrosc.* **2002**, *33*, 815−828.
(8) All crystals had a hexagonal needle morphology (typical dimensions 1 mm × 1 mm × 14 mm) with good optical quality.
(9) Harris, K. D. M.; Smart, S. P.; Hollingsworth, M. D. *J. Chem. Soc., Faraday Trans.* **1991**, *87*, 3423−3429.
(10) Experiments were performed with a Labram II spectrometer (Jobin-Yvon), an Ar/Kr 2018 Spectra-Physics laser (514.5 nm) and a grating of 1800 lines/mm (spectral resolution ca. 6 cm^{-1}). The laser was focused on the sample through a microscope (50x Olympus objective) of 0.55 numerical aperture and the diameter of the confocal pinhole was 700 μm. The radial and axial resolutions were 10 μm and 50 μm, respectively.
(11) Damen, T. C.; Porto, S. P. S.; Tell, B. *Phys. Rev.* **1966**, *142*, 570−574.
(12) The (100) face of the crystal[5b] was aligned parallel to the XY plane.
(13) (a) Smart, S. P.; El Baghdadi, A.; Guillaume, F.; Harris, K. D. M. *J. Chem. Soc., Faraday Trans.* **1994**, *90*, 1313−1322. (b) El Baghdadi, A.; Guillaume, F. *J. Raman. Spectrosc.* **1995**, *26*, 155−166.
(14) The average urea host structures in the DBO/urea and PD/urea inclusion compounds are essentially identical at ambient temperature.
(15) Hollingsworth, M. D.; Brown, M. E.; Hillier, A. C.; Santarsiero, B. D.; Chaney, J. D. *Science* **1996**, *273*, 1355−1359.

JA040117D